A New Approach of Two-Dimensional the NMR Relaxation Measurement in Flowing Fluid

Feng Deng · Lizhi Xiao · Guangzhi Liao ·
Fangrong Zong · Weiliang Chen

Abstract   Driven-equilibrium fast saturation recovery (DEFSR), as a new method for two-dimensional (2-D) nuclear magnetic resonance (NMR) relaxation measurement based on pulse sequence in flowing fluid, is proposed. The two-dimensional functional relationship between the ratio of transverse relaxation time to longitudinal relaxation time of fluid (T_1/T_2) and T_1 distribution is obtained by means of DEFSR with only two one-dimensional measurements. The rapid measurement of relaxation characteristics for flowing fluid is achieved. A set of the down-hole NMR fluid analysis system is independently designed and developed for the fluid measurement. The accuracy and practicability of DEFSR are demonstrated.

1 Introduction

The measurement technology for nuclear magnetic resonance (NMR) for flowing fluid has been studied as early as the 1950s; the first report of flow measurement by NMR was by Suryan [1], who used the fact that there was a rise in the signal when the fluid was flowing steadily with a uniform velocity. In 1990, Caprihan and Fukushima [2] conducted a detailed analysis of the influence of fluid flowing on the NMR signal. Then the methods for flow velocity distribution measurement and flow velocity profile imaging with NMR were proposed. In 1991, Callaghan elaborated on the NMR response of flowing fluid [3] in his work. Afterwards, a series of new theories and methods about the NMR application of the multiphase flow measurement have emerged in many fields such as chemistry, biology and medical treatment. In the research achievements mentioned above, the fluid analysis is carried out from the perspective of magnetic resonance imaging (MRI).

F. Deng · L. Xiao (✉) · G. Liao · F. Zong · W. Chen
State Key Laboratory of Petroleum Resources and Prospecting, College of Geophysics and Information Engineering, China University of Petroleum, 18 Fuxue Road, Changping, Beijing 102249, People's Republic of China
e-mail: xiaolizhi@cup.edu.cn

An NMR relaxation characteristic (longitudinal relaxation time T_1, transverse relaxation time T_2) is an inherent NMR response parameter, which is directly used for identifying fluid components [4]. In petroleum industry, the NMR relaxation measurement of flow is applied in the down-hole NMR fluid analysis system [5, 6]. The changes of NMR relaxation characteristics at different reservoir depths near the borehole can be monitored in real time on site. The two-dimensional (2-D) NMR relaxation characteristic (T_1–T_2) [7] is a common laboratory technique for describing the porous medium structure or fluid compositions. However, it takes a longer time to complete the T_1–T_2 measurement with the conventional method of the T_1-encoding pulse sequence [8]. Moreover, considering the signals with the low signal-to-noise ratio (SNR) acquired in the low-field environment, several sets of the data need to be accumulated after the multiple measurement, which further prolongs the measurement time. As fluid is constantly flowing within the detection domain of an NMR instrument, the long acquisition time is not suitable for the measurement of the relaxation property of the flowing fluid. Moreover, the Brownian movement of molecules of the flowing fluid is covered by the flowing movement during the process of flowing, which caused the diffusion coefficient increases [9], and accelerated the attenuation speed of the transverse magnetization vector. Therefore, T_2 cannot be accurately measured by the conventional Carr-Purcell-Meiboom-Gill (CPMG) pulse sequence under flowing state. In 2007, Kashaev et al. [10] proposed a rapid T_2 measurement method. Measurements of T_2 using this method last less than 2 s with appropriate accuracy. This method provides a good idea on measuring the 1-D T_2 distribution under flow state.

In 2009, Miechell et al. [11] proposed a driven-equilibrium (DE) CPMG pulse sequence which is a rapid method for obtaining the average ratio $<T_1/T_2>$ as a function of T_2. However, this method cannot be used to measure the flowing fluid, because it uses the CPMG pulse sequence to measure T_2, as mentioned above. In this article, we propose the DEFSR pulse sequence to measure the flowing fluid. The DEFSR pulse sequence, which consists two parts: an initial DE portion followed by a fast saturation recovery (FSR) portion, is shown in Fig. 1. The DE sequence is based on the driven-equilibrium Fourier transform (DEFT) pulse sequence [12]. DEFT allows the repeat acquisition of a spectrum without having to wait for the spins to recover on the longitudinal axis. This is achieved by applying a 180° radio-frequency (RF) pulse after a free induction decay (FID). When this process is repeated, the final magnetization vector tends to an equilibrium value M_{eq}, which contains the information about both T_1 and T_2 of the sample. The value of T_1/T_2 can be directly calculated by M_{eq}, this ratio combined with the T_1 distribution, which being measured by FSR pulse sequences, makes it possible to obtain the T_1/T_2–T_1 distribution. Since the DEFSR sequence is a 1-D experiment, the T_1/T_2 ratio distribution can be acquired in two scans. The 2-D relaxation measurement is much faster with the DEFSR pulse sequence than that with the conventional T_1-encoding pulse sequence. The measurement of T_2, which is quite sensitive to molecular diffusion, is replaced by that of T_1 which is insensitive to molecular diffusion. The DEFSR pulse sequence is effectively applied in the measurement of NMR relaxation under flowing state.

Crude oil usually contains asphaltene, which is a kind of a high-polymer compound. The content of the high-polymer compound results in the change of T_1/T_2. Therefore, the components of crude oil could be obtained by detecting the T_1/T_2 ratio. In this study, a method for analyzing the size of asphaltene polymer in crude
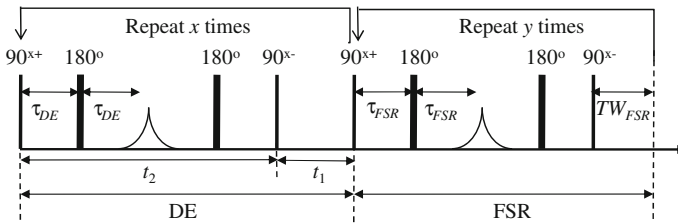
Fig. 1 DEFSR pulse sequence

oil with the DEFSR pulse sequence is proposed, which can provide some important technical references for the exploitation and transport of crude oil.

2 DEFSR Pulse Sequence

When the T_1-encoding pulse sequence is used to measure T_1–T_2, the polarization time (TW) should be arranged from 0 to $5T_1$. A set of CPMG pulse sequences is performed repeatedly with different TW, which takes much time. The T_1/T_2–T_1 distribution is obtained only by two scans with the DEFSR sequence proposed in this article (as shown in Fig. 1). DEFSR consists of one DE sequence, which is immediately followed by the FSR sequence. The measurement of the T_1/T_2 distribution is obtained by the rapid measurement within dozens of milliseconds to several seconds with the DE sequence; the T_1 distribution of the fluid is obtained by the fast measurement based on the improved saturation recovery.

2.1 Driven Equilibrium

As shown in Fig. 1, the DE sequence tips the magnetization vector in the longitudinal direction to the transverse direction. After a "truncated" CPMG echo train is collected within t_2, the DE sequence tips the magnetization vector in the longitudinal direction to the transverse direction. The polarization lasts for t_1. In this process, one 90° pulse and two 180° pulses are required to collect the echo signal. When the second echo signal is produced, the second 90° is pulse with the phase reverse to the first 90° pulse is used to tip the reunited magnetization vector to the longitudinal direction. This process is repeated for x times, until the final magnetization vector tends towards an equilibrium value M_{eq}, as in Fig. 2a. It should be noted that the values of t_1 and t_2 should be much smaller than T_1 and T_2 of the tested sample. This not only makes the approximate value of Eq. (1) closer to the real value, but also reduces the effect of diffusion and J-coupling [13] on the measurement result, which is very important for the flowing measurement.

It can be obtained that, after x times of the repeated process of the DE sequence, the magnetization vector of sample approaches the equilibrium value M_{eq}:

$$M_{eq} = M_0 \frac{1 - \exp(-\frac{t_1}{T_1})}{1 - \exp(-\frac{t_1}{T_1} - \frac{t_2}{T_2})} \approx M_0 \frac{1}{1 + \frac{T_1}{T_2}\frac{t_2}{t_1}}, \tag{1}$$
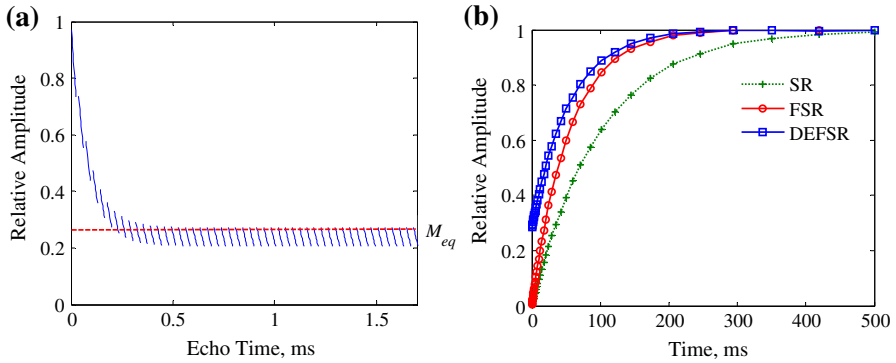
Fig. 2 Echo trains measured with the DEFSR pulse sequence in the numerical simulation: **a** DE pulse sequence measurement result, the *dashed line* show the value of M_{eq}; **b** FSR and DEFSR pulse sequence measurement result

where M_0 is the magnetization vector of the sample after complete polarization. The approximate expression is correct when t_1 and t_2 are much less than T_1 and T_2. According to Eq. (1), M_{eq} is only related to the T_1/T_2 ratio. Therefore, M_{eq} obtained by the measurement of the DE sequence is directly converted to the T_1/T_2 ratio of the sample. It should be noted that whether the sample contains a variety of relaxation components or not, the T_1/T_2 ratio obtained by the M_{eq} conversion is a single value, instead of a distribution. Thus, the DE sequence is not applicable to measuring multi-phase fluids which contain different components with several T_1/T_2 ratios such as crude oil. The FSR sequence is introduced in order to solve this problem.

Before the next step, it is necessary to quantify the sensitivity of the DE pulse sequence to offsets in the Larmor frequency ω_0 and RF inhomogeneities. In case of an ideal system, the M_{eq} value can be determined simply by applying the rotation matrices of the pulse to an initial Z-axis magnetization of M_0 and accounting for relaxation during the time t_1 and t_2. If there is an offset $\Delta\omega_0$ between the RF spin and nutation frequency ω_{rf} and the Larmor frequency $\gamma|B_0|$ (here γ is the gyromagnetic ratio and $|B_0|$ is the magnitude of the static magnetic field), we can get $\Delta\omega_0 \equiv \omega_{rf} - \gamma|B_0|$, and the actual nutation frequency of the spins will be given by:

$$\Omega = \sqrt{\Delta\omega_0^2 + \omega_1^2}, \tag{2}$$

where $\omega_1 = |B_1|/2\gamma$. Assuming the pulse duration t_p is much less than the average relaxation time $<T_1>$ and $<T_2>$, then the general rotation R can be determined by solving the Bloch equations without relaxation [14, 15]. A 90° pulse along the $\pm X$ axis is described by the rotation matrix:

$$R_{\pm 90x} = \begin{pmatrix} \cos\theta\cos^2\alpha + \sin^2 & \alpha - \sin\theta\cos\alpha & (1-\cos\theta)\sin\alpha\cos\alpha \\ \sin\theta\cos\alpha & \cos\theta & -\sin\theta\sin\alpha \\ (1-\cos\theta)\sin\alpha\cos\alpha & \sin\theta\sin\alpha & \cos\theta\sin^2\alpha + \cos^2\alpha \end{pmatrix}, \tag{3}$$

where θ is the rotation angle:

$$\theta \;=\; \frac{\Omega}{B_1}\frac{\pi}{2} \;\text{ and } \alpha \;=\; \tan^{-1}\frac{B_1}{\Delta B_0}. \tag{4}$$

To obtain the rotation matrix for a 180° pulse along the Y-axis, $\pi/2$ in the expression of θ is replaced by π. During free evolution periods, the magnetization simply precesses about the offset $\Delta\omega_0$, and the components of the magnetization after a time τ can be calculated as $M(t + \tau) = E \cdot M(t)$ [16], where:

$$E = \begin{pmatrix} \mathrm{e}^{-\tau/T_2}\cos\Delta\omega_0\tau & \mathrm{e}^{-\tau/T_2}\sin\Delta\omega_0\tau & 0 \\ \mathrm{e}^{-\tau/T_2}\sin\Delta\omega_0\tau & \mathrm{e}^{-\tau/T_2}\cos\Delta\omega_0\tau & 0 \\ 0 & 0 & e^{-\tau/T_1} \end{pmatrix}. \tag{5}$$

To include the new magnetization after a free evolution τ, a vector $M_{\mathrm{new}}(\tau) = (0,0,1-\exp(-\tau/T_1))$ must be added to the resultant magnetization at the end of the evolution period. In this way, after a free evolution τ, the magnetization is given by $M(t + \tau) = E \cdot M(t) + M_{\mathrm{new}}(\tau)$. Recalling $t_2 = 4\tau_{\mathrm{DE}}$, the magnetization vector of the $(x + 1)$th echo, m_{x+1}, will be given by:

$$m_{x+1} = [M(\tau_{\mathrm{DE}})R_{180y}M(\tau_{\mathrm{DE}})R_{+90x}M(t_1)R_{-90x}M(\tau_{\mathrm{DE}})R_{180y}]\{m_x\}. \tag{6}$$

Simulated data that illustrate the sensitivity of the DE pulse sequence to offsets in Larmor frequencies and RF inhomogeneities are shown in Fig. 3. Figure 3a demonstrates that, with homogeneous RF fields, since the maximum frequency offset Δf_0 considered here (2 kHz) is much smaller than the nutation frequency $\gamma|B_0|/2\pi = 34.7$ kHz, the pulses still act as near-perfect 90° and 180° pulses over the whole range. Figure 2b shows that, in the presence of significant RF inhomogeneities, at an RF inhomogeneity of $\pm 20\ \%$, the nominal 90° pulse transforms the transverse magnetization into the longitudinal magnetization and back imperfectly which will lead to a deviation in the resulting observed equilibrium magnetization M_{eq} from the ideal value, but when the precession of the transverse component during t_1 is close to an odd multiple of π, subsequent contributions tend to cancel and the observed value of M_{eq} is affected less by RF inhomogeneities. This occurs at offset frequencies $\Delta f_{0,i} = (i-1/2)/t_1$, where i is an integer. It is therefore preferable to perform the DE pulse sequence measurements at such offset frequencies.

2.2 Fast Saturation Recovery

The FSR pulse sequence can be used to measure the T_1 distribution rapidly, as shown in Fig. 1. The FSR pulse sequence is an application of the DE pulse sequence to the conventional saturation recovery (SR). The measurement speed of T_1 is increased about three times than SR (as shown in Fig. 2b). The FSR sequence tips the magnetization vector back to the longitudinal direction after each echo acquisition; the magnetization vector is stored for next polarization. This method saves the time for repeating polarization and provides a foundation for the T_1/T_2-T_1 distribution with DEFSR. FSR is different from DE which has fixed values of t_1 and t_2 for each scan. In FSR, the polarization time TW_{FSR} changes with the arrangement points, which is similar to the situation in SR. Within the range allowed by the equipment, the half inter-echo spacing τ_{FSR} in
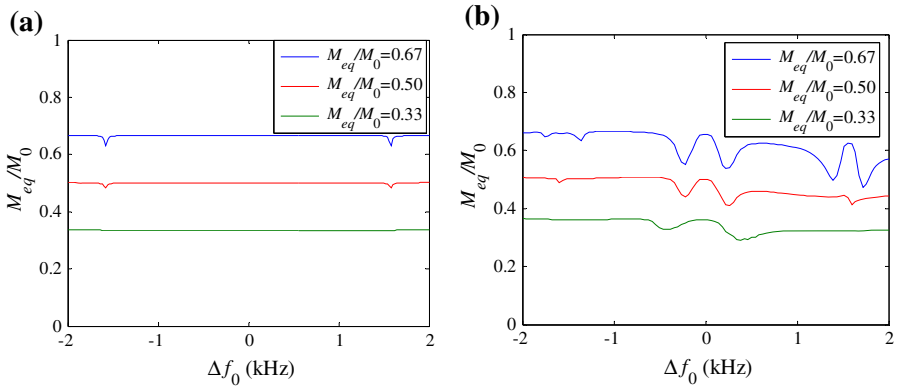
(a)

(b)

Fig. 3 Simulated variation in M_{eq}/M_0 generated by the DE pulse sequence as a function of rf frequency offset Δf_0. The calculations were performed assuming the following parameters: $T_1 = T_2 = 1,000$ ms, $x = 100$, SNR $= 100$, three curves show results for different values of t_2/t_1: 2/4 ms (*bottom*), 4/4 ms (*middle*) and 4/2 ms (*top*). **a** The rf field is uniform; **b** include a uniform distribution of B_1 between 80 and 120 % of its nominal value

FSR should be as short as possible. The effect of diffusion and *J*-coupling will be effectively reduced, while minimizing the attenuation of the magnetization vector in the transverse direction.

With the DEFSR sequence, re-polarization is necessary on the basis of M_{eq} obtained by the DE sequence, which is the reason for the unfitness of the SR pulse sequence. Assuming the sample contains only a single relaxation component, after polarization for $\mathrm{TW_{FSR}}$ with the FSR pulse sequence based on M_{eq}, the magnetization vector $M_{\mathrm{DEFSR}}(\mathrm{TW_{FSR}})$ of the fluid is shown as follows

$$M_{\mathrm{DEFSR}}(\mathrm{TW_{FSR}}) = M_{eq}\exp\left(-\frac{\mathrm{TW_{FSR}}}{T_1}\right) + M_0\left[1 - \exp\left(-\frac{\mathrm{TW_{FSR}}}{T_1}\right)\right]. \quad (7)$$

As discussed above, DEFSR requires two scans, one for the DEFSR sequence ("$M_{eq} + \mathrm{FSR}$") and one for the FSR pulse sequence beginning from the zero magnetization vector ("$0 + \mathrm{FSR}$"). In both scans, the same $\mathrm{TW_{FSR}}$ is used. The magnetization vector M_{FSR} of the sample after polarization for $\mathrm{TW_{FSR}}$ beginning from zero magnetization vector is given as follows:

$$M_{\mathrm{FSR}}(\mathrm{TW_{FSR}}) = M_0\left[1 - \exp\left(-\frac{\mathrm{TW_{FSR}}}{T_1}\right)\right]. \quad (8)$$

The relationship between the T_1/T_2 ratio and the magnetization vectors by two scans is obtained by a combination of Eq. (1), Eq. (7) and Eq. (8). It is shown in the following formula:

$$\frac{T_1}{T_2} = \frac{t_1}{t_2}\left[\frac{1 - M_{\mathrm{DEFSR}}(\mathrm{TW_{FSR}})}{M_{\mathrm{DEFSR}}(\mathrm{TW_{FSR}}) - M_{\mathrm{FSR}}(\mathrm{TW_{FSR}})}\right]. \quad (9)$$

In terms of the sample with a single relaxation component, T_1 of the sample is obtained by the Laplace transform [5, 16–18] of M_{FSR} ($\mathrm{TW_{FSR}}$). Hence, T_2 of the sample is obtained only by two scans with the DEFSR pulse sequence.

In an actual measurement, the tested sample is usually a mixture of multi-phase fluids with several relaxation components. In this case, the T_1/T_2–T_1 distribution or T_1–T_2 distribution cannot be obtained according to the relationship between *the T_1/T_2* ratio and the magnetization vector. The mathematical deduction is required.

We also need to quantify the sensitivity of "0 + FSR" and "M_{eq} + FSR" sequence to offsets in Larmor frequency ω_0 and rf inhomogeneities using the same method of Sect. 2.1. The numerical simulation results are shown in Fig. 4, with $t_1 = t_2 = 1$ ms, the correct observed echoes by DEFSR pulse sequence are obtained at an offset frequency of $\Delta f_0 = \pm 0.5$ kHz.

2.3 Distribution of Relaxation Time

In DEFSR, the changes of the magnetization vectors from two scans (M_{DEFSR} and M_{FSR}) with time TW_{FSR} are given by

$$M_{DEFSR,FSR}(TW_{FSR}) = M_{y=0} \exp\left(-\frac{TW_{FSR}}{T_1}\right) + M_0\left[1 - \exp\left(-\frac{TW_{FSR}}{T_1}\right)\right], \quad (10)$$

where $M_{y=0}$ is the initial magnetization vector of the measurement by the FSR sequence. When the sample is measured by "M_{eq} + FSR", $M_{y=0} = M_{eq}$. When the sample is measured by "0 + FSR", $M_{y=0} = 0$. When only the FSR measurement is carried out, the variation of the magnetization vector is quite simple. Only the changes of the magnetization vector measured by FSR are considered. By introducing the T_1 distribution into Eq. (10), the following expression is obtained:

$$M_{DEFSR}(TW_{FSR}) = \int d\log T_1 A_{DEFSR,FSR}(\log T_1) \exp\left(-\frac{TW_{FSR}}{T_1}\right)$$
$$+ M_0\left[1 - \exp\left(-\frac{TW_{FSR}}{T_1}\right)\right], \quad (11)$$

where $A_{DEFSR,FSR}(\log T_1)$ are the amplitude of T_1 distribution, which inversed from FSR results with two scans. Equation (11) can also be expressed in terms of the 2-D distribution function f_2 (log T_1, T_1/T_2):

$$M_{DEFSR}(TW_{FSR}) = \int\int d\log T_1 d\frac{T_1}{T_2} f_2\left(1 - \frac{M_{eq}}{M_0}\right) \exp\left(-\frac{TW_{FSR}}{T_1}\right)$$
$$+ M_0\left[1 - \exp\left(-\frac{TW_{FSR}}{T_1}\right)\right]. \quad (12)$$

Under normal circumstances, the T_1/T_2 distribution for fluid of a single component is confined within a very narrow band. So Eq. (12) is approximately expressed as follows:

$$M_{DEFSR}(TW_{FSR}) = \iint d\log T_1 f_1(\log T_1)\left(1 - \frac{M_{eq}}{M_0}\right) \exp\left(-\frac{TW_{FSR}}{T_1}\right)$$
$$+ M_0\left[1 - \exp\left(-\frac{TW_{FSR}}{T_1}\right)\right]. \quad (13)$$

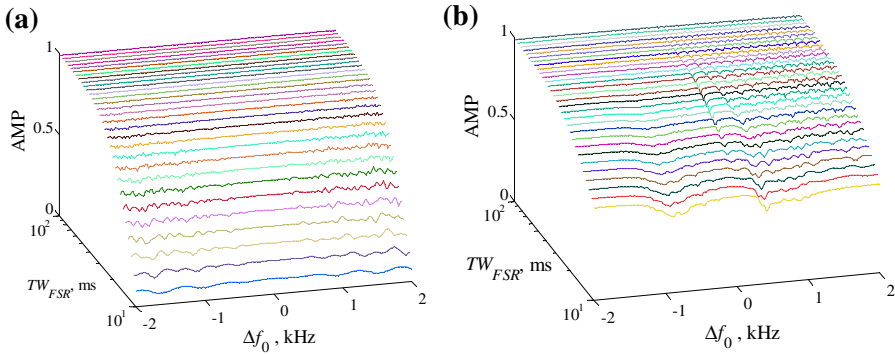By comparing Eqs. (11) and (13), the following formula is obtained:

Fig. 4 Numerical simulation in amplitude of echoes generated by "0 + FSR" and "M_{eq} + FSR" sequence as a function of rf frequency offset Δf_0 under nonuniform rf field. The calculations were performed assuming the following parameters: $T_1 = T_2 = 100$ ms, $x = 100$, $t_2 = t_1 = 1$ ms, SNR = 100. **a** "0 + FSR" sequence; **b** "M_{eq} + FSR" sequence

$$A_{\text{DEFSR}}(\log T_1) = f_1(\log T_1)\left(1 - \frac{M_{\text{eq}}}{M_0}\right), \tag{14}$$

where $f_1(\log T_1)$ is the 1-D distribution function of T_1. In addition, the T_1 distribution obtained by "0 + FSR" contains full distribution information of T_1, $A_{\text{FSR}}(\log T_1) = f_1(\log T_1)$. Thus, the following formula is obtained

$$\left\langle \frac{T_1}{T_2} \right\rangle_{T_1} = \frac{t_1}{t_2}\left[\frac{A_{\text{DEFSR}}(\log T_1)}{A_{\text{FSR}}(\log T_1) - A_{\text{DEFSR}}(\log T_1)}\right], \tag{15}$$

where $<T_1/T_2>_{T_1}$ is the function relating the T_1 distribution to the T_1/T_2 distribution. According to Eq. (15), the amplitude of the T_1 spectrum obtained by FSR of two scans can be used to deduce the T_1/T_2–T_1 distribution. From this, the T_1–T_2 distribution is obtained. Figure 5 shows the results of numerical simulation. The red equipotential line represents the T_1–T_2 distribution obtained by the T_1-encoding sequence measurement under the stationary state. The solid line represents the T_1–T_2 distribution obtained by DEFSR sequence measurement. A good consistency is found according the contrast observed.

3 Experiment

3.1 Equipment

In order to study and implement NMR relaxation measurements under flowing state, a down-hole NMR fluid analysis system is produced [5]. The appearance of this equipment is shown in Fig. 6. The down-hole NMR fluid analysis system is mainly used for detecting ^{1}H NMR relaxation characteristics of reservoir fluid. The magnetic field strength of the detection area is 533 G; the radio frequency is $f_0 = 2.2$ MHz. The equipment is designed with "outside-in" magnetic field. A ring-

Fig. 5 T_1–T_2 distribution obtained by DEFSR pulse sequence measurement through numerical simulation
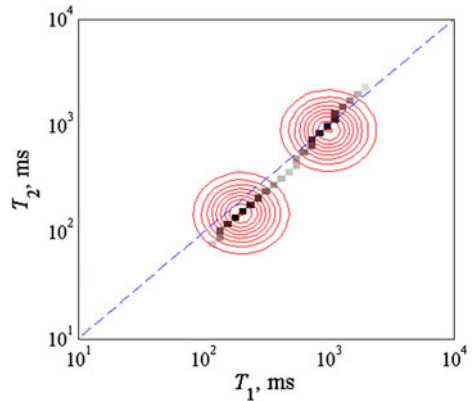
shaped magnet is used, and the fluid sample flows through the center of the magnet. The NMR measurement is carried out in flowing fluid. The equipment consists of three magnet segments, the first two of which are for prepolarization. The purpose is to ensure that the fluid is completely polarized when it flows into the detection area. The third magnet segment is to provide the static magnetic field required by NMR response of the fluid. The pipe through which the fluid passes in the detection area has an inner diameter of 25 mm. The flow velocity is controlled by a piston.

The down-hole NMR fluid analysis system is operated in flowing fluid. During the NMR signal acquisition, the DEFSR sequence repeatedly flips the magnetization vector between transverse and longitudinal directions. If the traditional single coil is used, the fluid passing through the signal acquisition area will change due to its flowing movement, causing magnetization vector disorder [18]. Thus, the antenna structure should be properly designed to ensure the accuracy and integrity of the acquired signals. The down-hole NMR fluid analysis system is equipped with a separate antenna structure, as shown in Fig. 7. Pulse emission and signal reception are undertaken by two separate antennas. The conventional spiral coil is used as an emitting antenna, which has the length of $A_1 = 400$ mm. The saddle coil is used as receiving antenna, with the length of $A_2 = 100$ mm. Two different coil structures will avoid the coupling between two antennas in signal acquisition, which is conducive to improving the SNR ratio. The tail ends of the two antennas are aligned. The fluid does not enter into the receiving antenna until sometime after it enters into the emitting antenna. In this way, the emitted pulse sequence will excite the fluid within the entire A_1 region. The received signal is only the echo signal within the A_2 region. As long as the distance by which the fluid flows within the entire DEFSR pulse sequence does not exceed $A_1 - A_2$, the magnetization vector disorder due to flow velocity would not occur.

3.2 Results and Discussion

To demonstrate the accuracy and practicability of DEFSR pulse sequence, the flow measurement experiment is first carried out using the down-hole NMR fluid analysis system over fluid sample of single component (distilled water and $CuSO_4$ solution). T_1 distributions, $T_1/T_2 - T_1$ distribution and $T_1 - T_2$ distribution obtained by two scans are
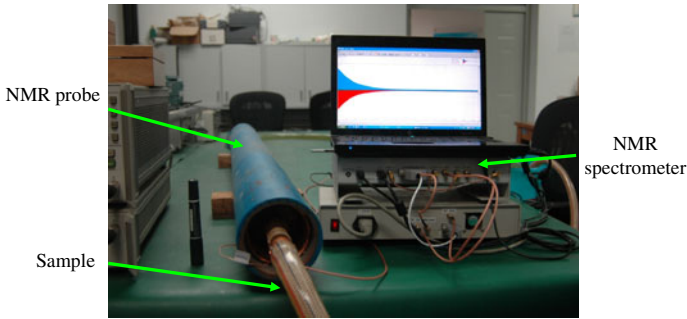
Fig. 6 Photo of the down-hole NMR fluid analysis system

shown in Fig. 8 from top to bottom, the experimental parameters are: TW_{FSR} arranged from 0.5 to 1000 ms, $f_0 = 2.2$ MHz, SNR $= 100$, $v = 5$ ml/s, $x = 10$, $y = 30$, $t_1 = t_2 = 500$ ms for the distilled water experiment and $t_1 = t_2 = 50$ ms for the distilled water experiment. According to the results, the T_1/T_2 distribution measured with the DEFSR sequence shows good consistency with that measured by the traditional the T_1-encoding sequence. For fluid with the longer relaxation time, it takes longer for the DE pulse sequence to drive the magnetization vector to the equilibrium value. Moreover, the DE pulse signal is more affected by the flow velocity, which is unfavorable for the flow velocity measurement.

Next, the experiments with crude oil samples that have three different viscosities and multiple relaxation components were carried out. The results are shown in Fig. 9, the experimental parameters are: TW_{FSR} arranged from 0.5 to 1000 ms, $f_0 = 2.2$ MHz, SNR $= 100$, $x = y = 30$, $t_1 = t_2 = 50$ ms. High-viscosity crude oil is usually in solid state under normal temperature and pressure. The measurement accuracy of fluid with the faster relaxation time is higher than that of fluid with the lower relaxation time. For this reason, the crude oil sample is not measured in free-flowing state. The sample is placed into a sealed tube, which is equipped with a detector for the measurement. The results indicate that the T_1/T_2 distribution of multi-component fluid measured with the DEFSR pulse sequence agrees well with that measured by the T_1-encoding pulse sequence also, but the precision of the DEFSR is lower than that of the T_1-encoding. Due to the measurement with DEFSR sequence requires frequent emission of high-frequency pulses, the antenna circuit should be properly protected.

4 Application

Asphaltenes are an important ingredient of crude oil because they can easily aggregate and affect the rheological properties of the fluid. Their aggregation not only poses interesting scientific problems but also has great economic significance because asphaltene precipitation can clog reservoir formation and production pipelines, which have bad influence in the production process [19, 20].

Asphaltene molecules easily aggregate and act as relaxation contrast agents. The asphaltene aggregates form large structures which introduce motion, slow as
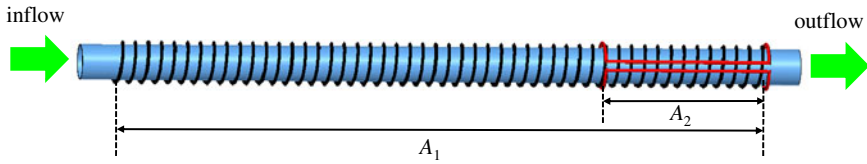
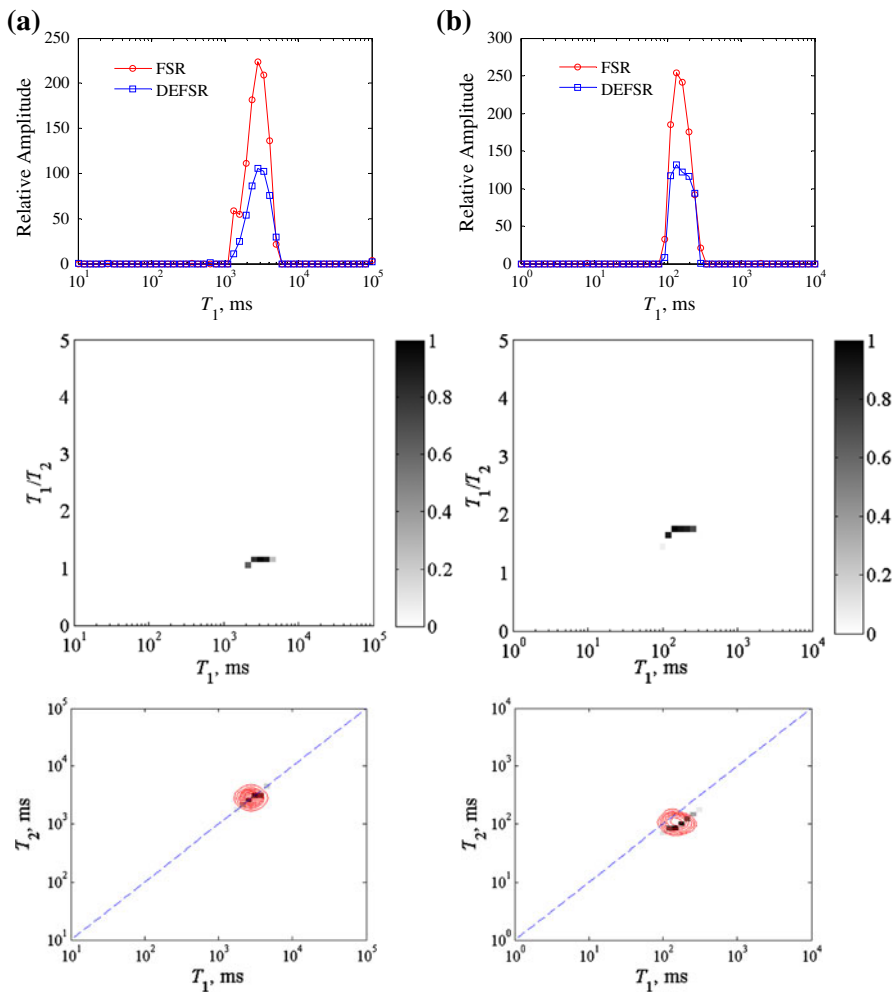**Fig. 7** Schematic diagram of separate antenna structure

Fig. 8 Measurement results of single-component fluid sample: from top to bottom, respectively T_1 distribution, T_1/T_2–T_1 distribution and T_1–T_2 distribution **a** distilled water, flow velocity $v = 5$ ml/s, $t_1 = t_2 = 500$ ms, $x = 10$, $y = 30$; **b** CuSO$_4$ solution, $v = 5$ ml/s, $t_1 = t_2 = 50$ ms, $x = 10$, $y = 30$

compared to the Larmor frequency, causing $T_1/T_2 > 1$. Additionally, high-viscosity (η) oils can have complicated T_1 and T_2. The effective rotational correlation time, τ_c, in a molecule is a key parameter for NMR in solution [21]. τ_c usually correlates to a good
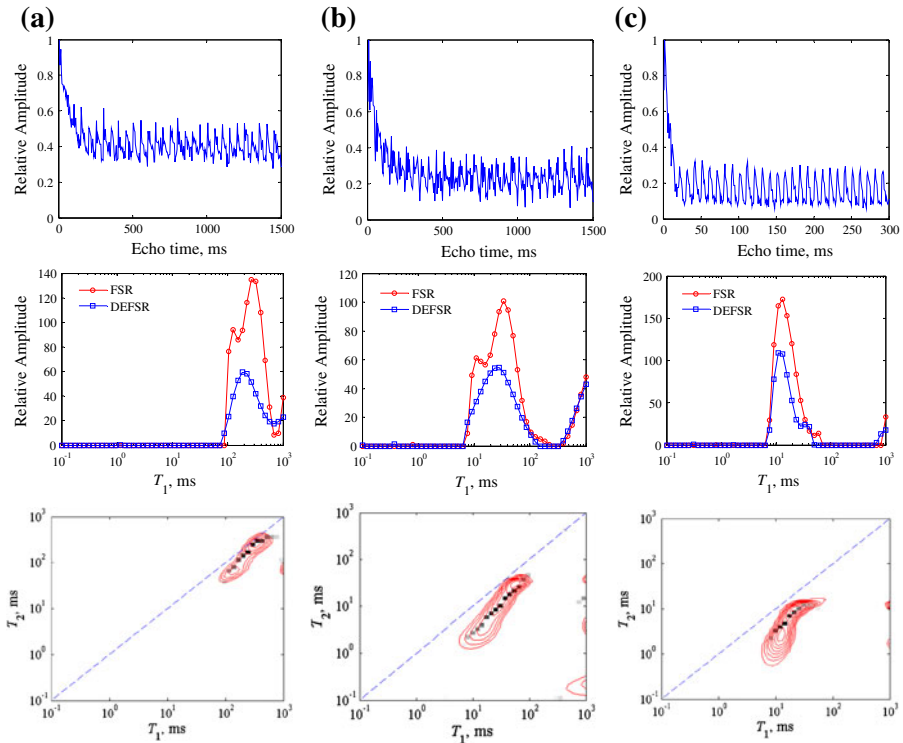
Fig. 9 Measurement results of multi-component samples: **a** low-viscosity crude oil with 1.99 % asphaltene content, $t_1 = t_2 = 50$ ms, $x = 30$, $y = 30$; **b** middle-viscosity crude oil with 6.99 % asphaltene content, $t_1 = t_2 = 50$ ms, $x = 30$, $y = 30$; **c** high-viscosity crude oil with 10.51 % asphaltene content, $t_1 = t_2 = 50$ ms, $x = 30$, $y = 30$

approximation with the molecular weight, and can, for example, indicate if aggregates are formed under the chosen conditions. Knowledge of the τ_c has certain functions with T_1 and T_2 [22, 23]. After a simple mathematical derivation, the correlation of T_1/T_2 and τ_c can be obtained:

$$\frac{T_1}{T_2} = \frac{1}{2} \frac{5(1 + \omega^2 \tau_c^2)^{-1} + 2(1 + 4\omega^2 \tau_c^2)^{-1} + 3}{(1 + \omega^2 \tau_c^2)^{-1} + 4(1 + 4\omega^2 \tau_c^2)^{-1}}, \qquad (16)$$

here $\omega = 2\pi f$ where f is the ^{1}H frequency. Within Eq. (16), τ_c can be extracted from the measured T_1/T_2 ratio. Figure 10 shows the relationship between the T_1/T_2 ratio and τ_c at 2.2 MHz. The T_1/T_2 ratio increases with τ_c. Comparing Eq. (15) and Eq. (16), the τ_c distribution is estimated based on the T_1/T_2 distribution of crude oil samples. Figure 11 shows the experimental τ_c distribution of the three crude oil samples. It is a good application to predict the η of a fluid sample using the Stokes–Einstein relation [24, 25]:
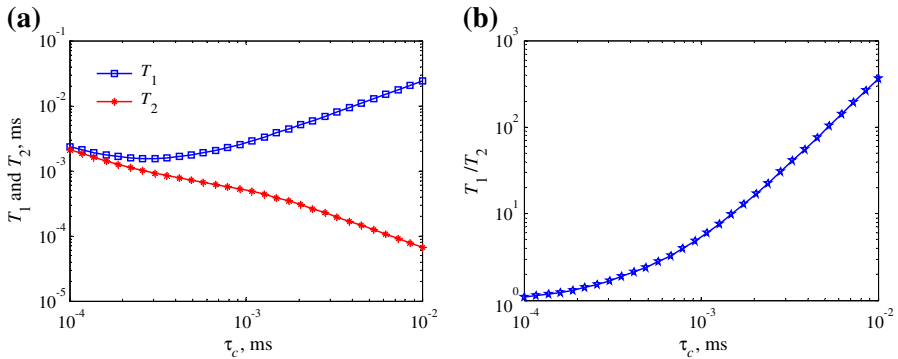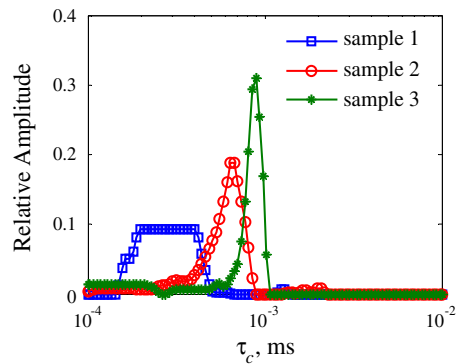
$$\tau_c = \frac{4\pi \eta a^3}{3kT}, \qquad (17)$$

(a)

(b)

Fig. 10 Relationship between relaxation time and τ_c at Larmor frequency of 2.2 MHz: **a** relationship between T_1, T_2 and τ_c; **b** relationship between T_1/T_2 and τ_c

Fig. 11 Experimental τ_c distribution of the three crude oil samples with different η: the η of sample 1, sample 2 and sample 3 is 57.5 cp, 230.6 cp and 897.4 cp respectively

where k is the Boltzmann constant, T is temperature and a is associated with the molecular size of sample. For crude oil samples, the parameter a is close to a constant, 4.3×10^{-7} mm.

5 Conclusion

The DEFSR pulse sequence can be used to rapidly measure the relaxation times of flowing fluid. The measurement results with DEFSR and its application methods are analyzed. It is found that DEFSR has the following advantages:

1. DEFSR only requires two scans (one measurement of the DEFSR pulse sequence and one measurement of the FSR pulse sequence). Based on this, the 2-D relaxation time distribution of the sample could be known. The measurement speed is much faster than the T_1-encoding pulse sequence.
2. DEFSR is mainly applicable to T_1 measurement which is insensitive to molecular diffusion. Thus, the accurate measurement of fluid relaxation characteristics at the flowing state is implemented.

3. The T_1/T_2 distribution of fluid can be used to directly deduce the distribution of time of fluid molecule realignment. Therefore, the method of DEFSR can be widely applied in the industrial process of dynamic monitoring such as composition identification of reservoir crude oil, process monitoring of chemical reaction, transport pipe monitoring, and water quality monitoring.

However, the application of the DEFSR pulse sequence has still some limitations. The DEFSR pulse sequence can be used to quickly determine the relationship between the T_1/T_2 ratio and the T_1 distribution, based on which the 2-D T_1–T_2 distribution is estimated. The resolution and precision of the T_1–T_2 distribution with DEFSR are inferior to those by the T_1-encoding pulse sequence. In addition, the DEFSR pulse sequence measures the fluid relaxation characteristics under flowing state. However, the maximum value of the flow velocity of the fluid that can be measured is restricted by the antenna length. So far the rapid measurement is not possible with fast-flowing fluid.

References

1. J.R. Suryan. Proc. Indian Acad. Sci. Sect. A **33**, 107–111 (1951)
2. A. Caprihan, E. Fukushima. Phys. Rep. **198**, 195–235 (1990)
3. P.T. Callaghan. Oxford: Clarendon, p. 492
4. G.R. Coats, L.Z. Xiao, M.G. Prammer, *NMR Logging Principles and Applications* (Gulf Professional Publishing, Houston, 1999)
5. B.S. Wu, L.Z. Xiao, X. Li, H. J. Wu, T. L. An. Petrol. Sci. **9**(1), 38–45 (2012)
6. M.G. Prammer, J.C. Bouton, P. Masak. US 20050017715A1. 2005-01-27
7. Y.Q. Song, L. Venkataramanan, M.D. Hürlimann, M. Flaum, P. Frulla, C. Straley. J. Magn. Reson. **154**, 261–268 (2002)
8. M.D. Hürlimann, L. Venkataramanan. J. Magn. Reson. **157**, 31–42 (2002)
9. J. Bouton, M.G. Prammer, P. Masak, S. Menger. Louisiana: SPE annual technical conference and exhibition, EP 1108225 A1 (2001)
10. R.S. Kashaev, A.N. Teмnikov, Z.Sh. Idiyatullin, I.R. Dautov. Patent of Russian Federation No. 74710, G01N24/08, 2007 (in Russian)
11. J. Mitchell, M.D. Hürlimann, E.J. Fordham. J. Magn. Reson. **154**, 261–268 (2009)
12. E.D. Becker, J.A. Ferretti, T.C. Farrar. J. Am. Chem. Soc. **91**, 7784–7785 (1969)
13. H.T. Edzes. J. Magn. Reson. **17**, 301–303 (1975)
14. F. Bloch. Phys. Rev. **70**, 460–474 (1946)
15. M.D. Hürlimann, D.D. Griffin. J. Magn. Reson. **143**, 120–135 (2000)
16. F. Casanova, J. Perlo, B. Blümich, *Single-sided NMR* (Springer, New York, 2011)
17. R.J.S. Brown. J. Magn. Reson. **82**, 539–561 (1989)
18. Z.F. Zhang, L.Z. Xiao, G.Z. Liao, H.B. Liu, W. Xu, Y. Wu, S.J. Jiang. Appl. Magn. Reson. (2013)
19. H.B. Liu, L.Z. Xiao, H.J. Yu, X. Li, B.X. Guo, Z.F. Zhang, F.R Zong, A. Vladimir, S. Anferova. Appl. Magn. Reson. (2013). doi:10.1007/s00723-012-0415-9
20. F. Deng, L.Z. Xiao, H.B. Liu, T.L. An, M.Y. Wang, Z.F. Zhang, W. Xu, J.J. Cheng, Q.M. Xie, A. Vladimir. Appl. Magn. Reson. **44**, 1053–1065 (2013)
21. L. Zielinski, I. Saha, D.E. Freed, M.D. Hürlimann. Langmuir **26**(7), 5014–5021 (2010)
22. D.E. Freed, M.D. Hürlimann. C. R. Phys. **11**, 181–191 (2010)
23. D.H. Lee, C. Hilty, G. Wider, K. Wüthrich. J. Magn. Reson. **17**, 72–76 (2005)
24. A. Abragam, *Principles of Nuclear Magnetic Resonance* (Oxford Science Publications, Oxford, 1989)
25. D.M. Wilson, G.A. LaTorraca. Symposium of Society of Core Analysts. 1999, Paper 9923